

1    **SUPPLEMENTARY INFORMATION**

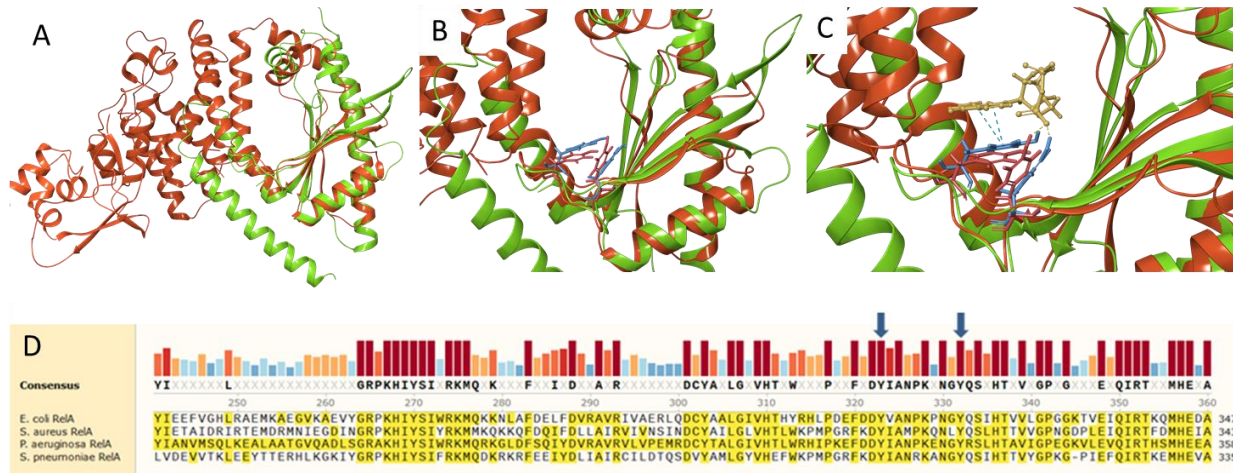
2    **The Development of a Pipeline for the Identification and Validation of Small-Molecule RelA  
3    Inhibitors for Use as Anti-biofilm Drugs**

4    *Donald C. Hall Jr<sup>1,2</sup>, Jarosław E. Król<sup>2</sup>, John P. Cahill<sup>1</sup>, Hai-Feng Ji<sup>1#</sup>, Garth D. Ehrlich<sup>2,3#</sup>*

5    *<sup>1</sup>Department of Chemistry; <sup>2</sup>Center for Advanced Microbial Processing, Center for Genomic Sciences,  
6    Center for Surgical Infections and Bacterial Biofilms, Institute of Molecular Medicine and Infectious  
7    Disease; Department of Microbiology & Immunology; <sup>3</sup>Department of Otolaryngology-Head and Neck  
8    Surgery; Drexel University College of Medicine, Drexel University, Philadelphia, PA*

9    #: Corresponding Authors

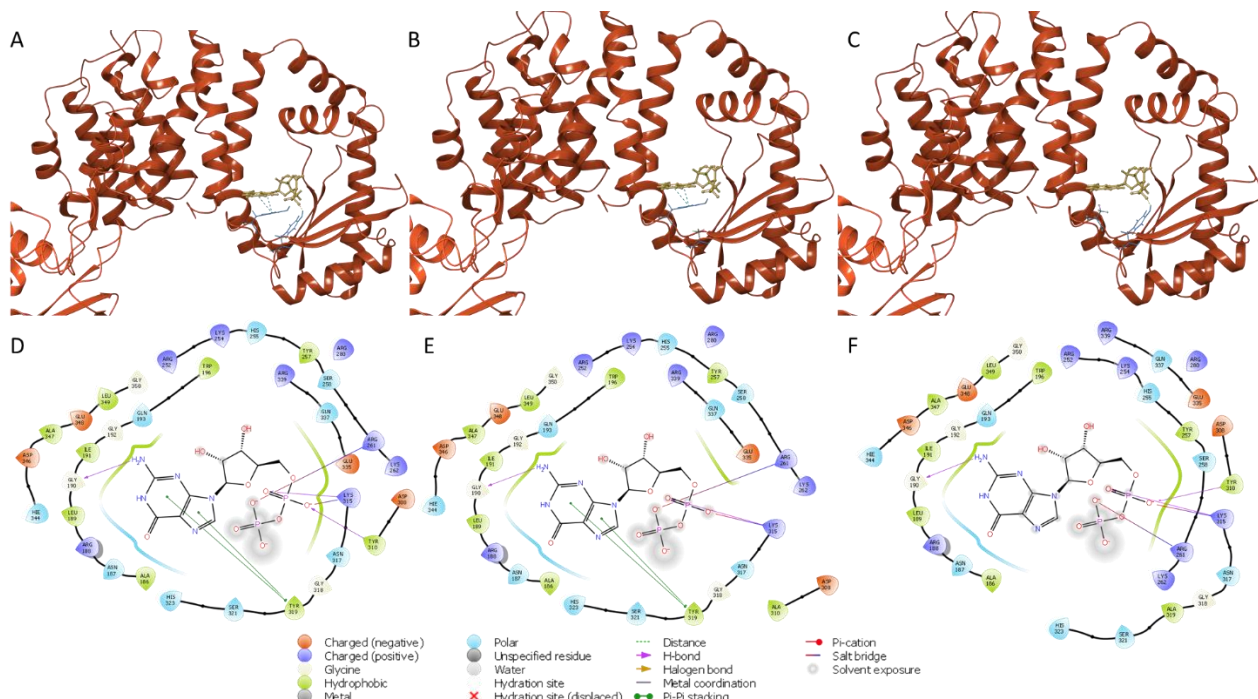
10



11

12 **Figure S1. RelA structure and sequence homology.** A) Structural alignment of known active site of *S.*  
13 *aureus* RelP (green) with *E. coli* RelA (orange); B) Alignment of *S. aureus* RelP (green) with *E. coli* RelA  
14 (orange) with two essential amino acids residues shown; C) GDP interactions with the essential residues  
15 can be seen with H-bonding and π-stacking shown in dashed lines; D) Protein sequence alignment of  
16 selected bacterial species (both Gram-positive and Gram-negative). Arrows denote conservation of the  
17 essential residues shown in B among most bacterial species shown

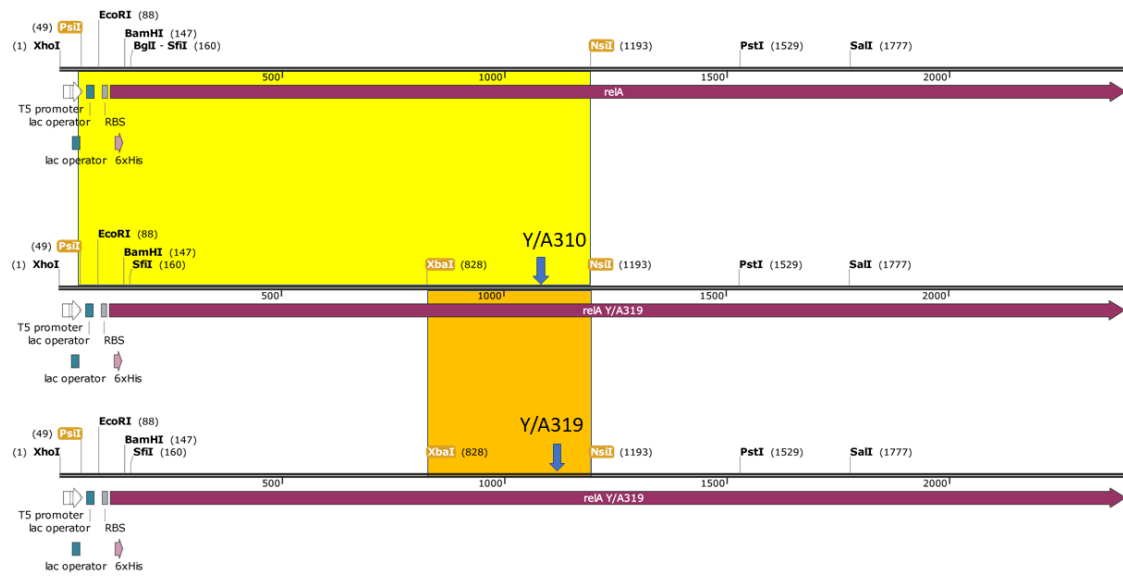
18



19

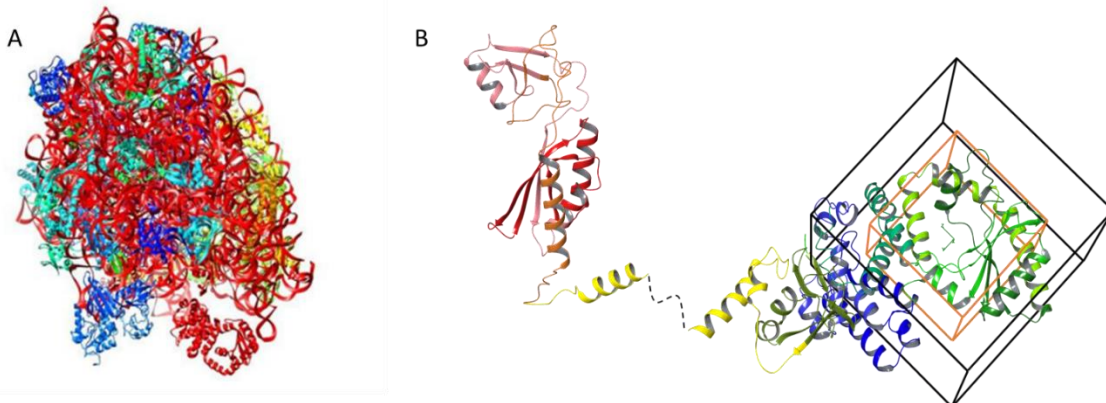
20 Figure S2. **RelA GDP interactions with and without amino acid mutations.** (A) 3D native RelA  
21 interaction (B) 3D Y/A-310 GDP interaction (C) 3D Y/A-319 GDP interaction (D) 2D native RelA  
22 interaction (E) 2D Y/A-310 GDP (F) 2D Y/A-319 GDP

23



24

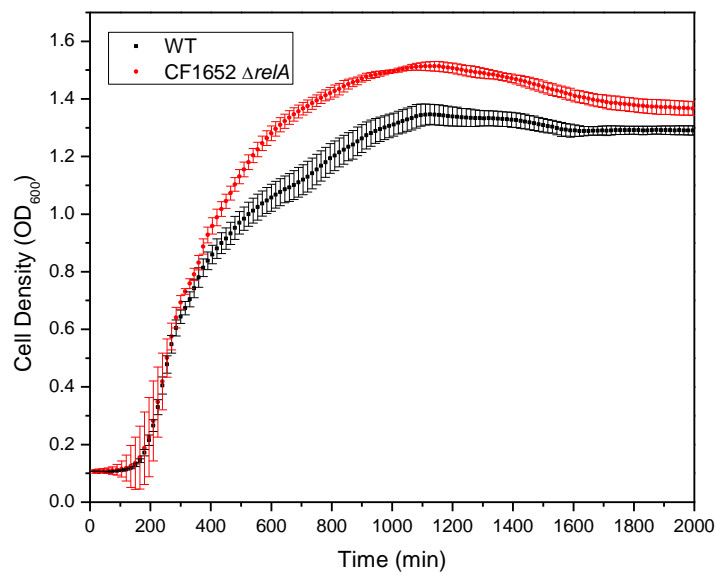
25 Figure S3. **RelA amino acid mutation scheme.** Arrows indicate where the mutation was introduced in the  
26 *relA* expression plasmid.



27

28 Figure S4. **Raw Cryo-EM structure of RelA (PDB: 5IQR).** RelA bound to a ribosome (A) and optimized  
29 RelA structure with docking grid box shown (B).

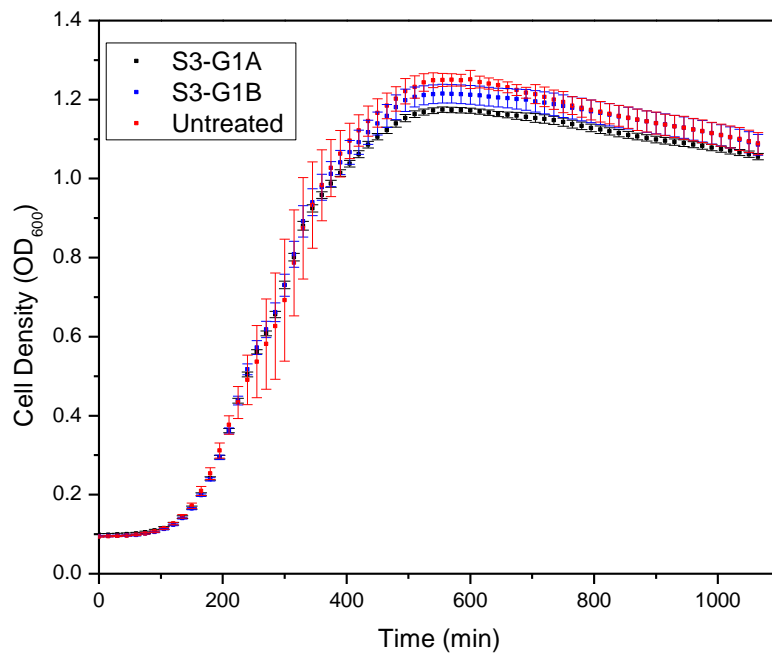
30



31

32 Fig S5. **Effect of *relA* and *relA/spoT* mutations.** Overnight growth curves of Wild Type *E. coli* and the  
33 CF1652  $\Delta$ relA mutant.

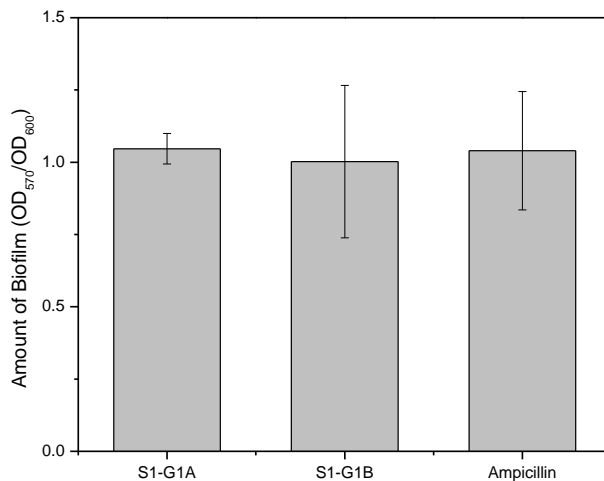
34



35

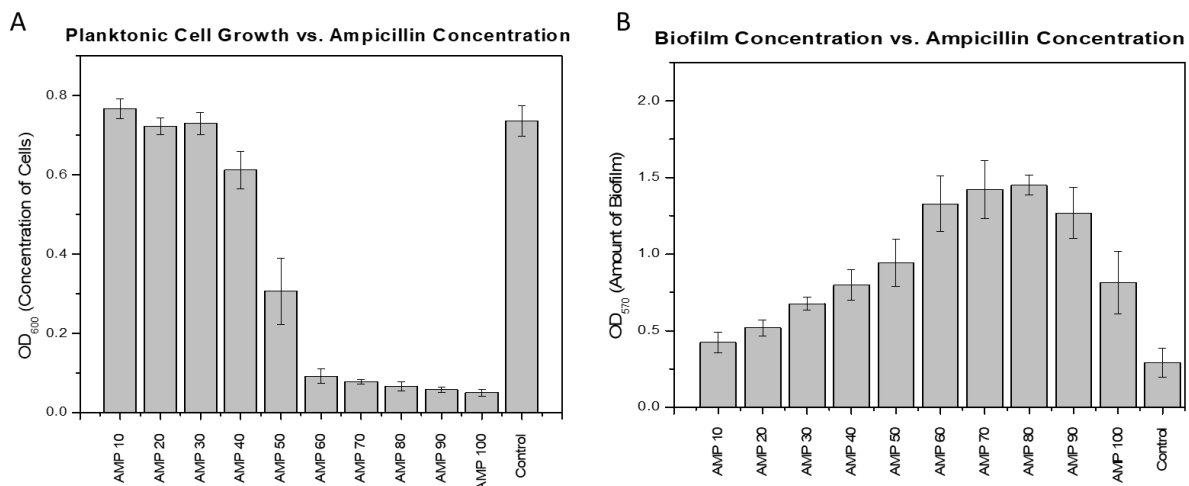
36 Figure S6. Compound effect on planktonic growth of *E. coli* C. *E. coli* C treated with compounds S3-  
37 G1A and S3-G1B ( $30 \mu\text{g}\cdot\text{mL}^{-1}$ ).

38



39

40 Figure S7. Effect of compounds on inhibition of *E. coli* C biofilm. S3-G1A and S3-G1B effect on the  
41 formation of biofilms using the crystal violet quantification method.



42

43 Figure S8. Effect of ampicillin concentration on planktonic and biofilm growth. A) Growth of cells in  
44 liquid culture at various concentrations of ampicillin ( $\text{OD}_{600}$ ). B) Amount of biofilm formed at various  
45 concentrations of ampicillin. (AMP# = AMP at #  $\mu\text{g}\cdot\text{mL}^{-1}$  concentration)

46 Table S1. **Bacterial strains and plasmids utilized in this work.** WT = wild type; Km = kanamycin; Cm  
47 = chloramphenicol

Strain and plasmid	Phenotype	Source
<i>E. coli</i> K12 MG1655	WT	Lab collection
<i>E. coli</i> C	WT	Lab collection
<i>E. coli</i> AG1 (ME5305)	F <sup>-</sup> , <i>recA1 endA1 gyrA96 thi-1 hsdR17(r<sub>k</sub><sup>-</sup> m<sub>k</sub><sup>+</sup>) supE44 relA1</i>	Kitagawa, M. et al.
<i>E. coli</i> CF1648	WT	M. Cashel
<i>E. coli</i> CF1652	<i>relA::Km</i>	M. Cashel
<i>E. coli</i> CF1693	<i>relA::Km, spoT::Cm</i>	M. Cashel
pJW2755-AM	pCA24N(GFP-) with <i>relA</i> gene ASKA plasmid, Cm <sup>R</sup>	Kitagawa, M. et al.
pJEK2020-43	pJW2755AM with <i>Xba</i> I silent site and Y/A319 mutation	This work
pJEK2020-20	pJW2755AM with <i>Xba</i> I silent site and Y/A310 mutation	This work

48

49